

# Identification of yield locus parameters of metals using inverse modeling and full field information

D. Lecompte<sup>1</sup>, S. Cooreman<sup>2</sup>, H. Sol<sup>2</sup>, J. Vantomme<sup>1</sup>, L. Rabet<sup>1</sup>, A.M. Habraken<sup>3</sup>

<sup>1</sup> Department of Materials and Construction, Royal Military Academy  
Av. De la Renaissance 30, 1000 Brussel, Belgium

<sup>2</sup> Mechanics of Materials and Constructions, Vrije Universiteit Brussel  
Pleinlaan 2, 1050 Brussels, Belgium

<sup>3</sup> Mechanics of Materials and Structures, Université de Liège,  
Chemin des Chevreuils 1, 4000 Liège, Belgium

email : david.lecompte@rma.ac.be; stcoorem@vub.ac.be; hugos@vub.ac.be

**Abstract:** The basic principle of the inverse modeling procedure as it is used for parameter identification is the generation of a complex and heterogeneous deformation field that contains as much information as possible about the parameters to be identified. One way of obtaining such a non-homogeneous deformation is by making the geometry of the specimen less regular. Another possibility is to make the loading conditions more complex. In this paper both options are actually combined by using the concept of a biaxial tensile test on a perforated cruciform specimen. In the present paper, the work hardening of the material is assumed to be isotropic and it is described by a Swift law. The yield locus is modeled by the anisotropic Hill48 criterion. The optimization technique used is a constrained gradient based Newton-type routine, which means that in every iteration step, a sensitivity calculation has to be performed in order to indicate the direction in which the parameters are to be optimized. The functional to be minimized is a least-squares expression of the discrepancy between the measured and the simulated strain fields at a certain load. The numerical routines as well as the identification results of the different parameters, based on simulated strain fields, are discussed.

**Keywords:** inverse modeling, Swift hardening law, Hill48 yield surface, full-field strain information

## I. INTRODUCTION

The accuracy of a Finite Element Simulation for plastic deformation strongly depends on the chosen constitutive laws and the value of the material parameters within these laws. The identification of those mechanical parameters can be done based on homogeneous stress and strain fields such as those obtained in uni-axial tensile tests and simple shear tests performed in different plane material directions. Another way to identify plastic material parameters is by inverse modeling of an experiment exhibiting a heterogeneous stress and strain field. Material parameter identification methods, which integrate optimization techniques and numerical methods such as the finite element method (FEM), indeed offer an alternative tool. The most common approach is to determine the optimal estimates of the model parameters by minimizing a selected measure-of-fit between the responses of the system and the model [1-3]. In the present study a method is proposed for the identification of the initial yield stress, the two parameters of a Swift isotropic hardening law and the four parameters of the Hill48 yield surface, based on the full-field surface measurements of a cruciform specimen subjected to biaxial tensile loading. Experimental forces and strains are

in this case compared to the simulated values. A finite element model of the perforated specimen serves as numerical counterpart for the experimental set-up. The difference between the experimental and numerical strains ( $\epsilon_x$ ,  $\epsilon_y$  and  $\epsilon_{xy}$ ) is minimized in a least squares sense by updating the values of the different parameters simultaneously. The sensitivities used to obtain the parameter updates are determined by finite differences, using small parameter perturbations. The optimization routine used, is based on a constrained Newton-type algorithm.

Paragraph two gives a description of the experimental equipment that will be used for the actual tensile testing of the cruciform specimens. In paragraph three, some information is given about the choice of the numerical model. Paragraph four talks about traditional elasto-plastic material identification, whereas paragraph five concerns the numerical aspects of the optimization routine and the sensitivity analysis used in the inverse modeling procedure for parameter identification. And finally, paragraph six shows some results obtained based on simulated strain fields.

## II. BIAXIAL TESTING

Different experimental techniques and specimens have been used to produce biaxial stress states. These techniques may be mainly classified into two categories [4]: (i) tests using a single loading system and (ii) tests using two or more independent loading systems. In the first category the biaxial stress ratio depends on the specimen geometry—their main disadvantage—, whereas in the second category it is specified by the applied load magnitude. Examples of the first category are bending tests on cantilever beams, anticlastic bending of rhomboidal shaped plates and bulge tests. Examples of the second category are thin-walled tubes subjected to a combination of tension/compression with torsion or internal/external pressure, and cruciform specimens under biaxial loading [5]. The most realistic technique to create biaxial stress states consists of applying in-plane loads along two perpendicular arms of cruciform specimens. The use of hydraulic actuators represents a very versatile technique for the application of the loads. The main difference between the existing techniques is the use of one or two actuators per loading direction. One actuator per loading direction [6] will cause movements of the centre of the specimen causing a side bending of the specimen. This results in undesirable non-symmetric strains. Systems with four actuators [7] with a

close-loop servo control using the measured loads as feedback system, allow the centre of the specimen standing still.

The plane biaxial test device using cruciform specimens developed at the Free University of Brussels has four independent servo-hydraulic actuators with an appropriate control unit to keep the centre of the specimen explicitly still. The device (Figure 1) has a capacity of 100 kN in both perpendicular directions, but only in tension. As no cylinders with hydrostatic bearing were used, failure or slip in one arm of the specimen will result in sudden radial forces which could seriously damage the servo-hydraulic cylinders and the load cells. To prevent this, hinges were used to connect the specimen to the load cells and the servo-hydraulic cylinders to the test frame. Using four hinges for each loading direction results in an unstable situation in compression and consequently only tension loads can be performed.

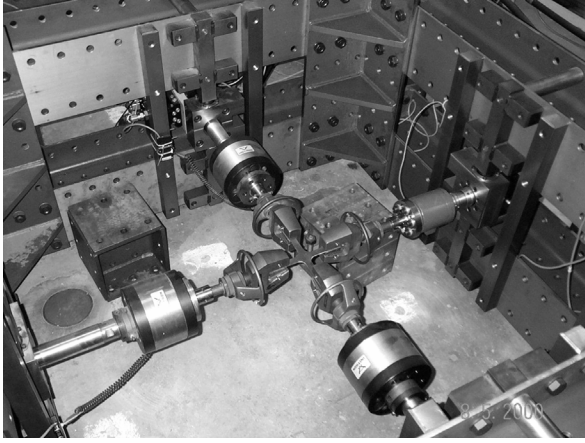


Figure 1: Plane biaxial test device for cruciform specimens

In an ideal situation no displacement of the centre point of the specimen is observed. Even when using four actuators, a small displacement might occur in a real situation. However, it is possible to quantify this small load difference and to use this as a control signal.

This type of experiment has already been used in the past for the identification of the elastic orthotropic parameters of composite materials [8].

### III. NUMERICAL MODELING

#### A. Constitutive model

The first assumption made, concerning the material model used, is that it exhibits rate independent elasto-plastic behaviour. Furthermore the elastic part is assumed to be linear and isotropic. The constitutive law used in the FE-formulation is based on a hypoelastic-plastic model, assuming the additive decomposition of the total strain into a reversible elastic part  $\varepsilon^{el}$  and an irreversible plastic part  $\varepsilon^{pl}$ . In rate form this condition becomes:

$$\dot{\varepsilon} = \dot{\varepsilon}^{el} + \dot{\varepsilon}^{pl} \quad (1)$$

The stress rate is always related to the elastic strain rate by means of the elastic moduli E:

$$\dot{\sigma} = E : \dot{\varepsilon}^{el} = E : (\dot{\varepsilon} - \dot{\varepsilon}^{pl}) \quad (2)$$

For the determination of the plastic strain rate, an associative flow rule is used:

$$\dot{\varepsilon}^{pl} = \dot{\lambda} \frac{\partial \Phi}{\partial \sigma} \quad (3)$$

in which  $\dot{\lambda}$  is the plastic multiplier and  $\Phi$  is the yield function. This plastic multiplier can be determined using the loading-unloading conditions:

$$\dot{\lambda} \geq 0 ; \Phi \leq 0 ; \dot{\lambda} \Phi = 0 \quad (4)$$

#### B. Yield surface shape

The yield function  $\Phi$  which governs the onset and continuance of plastic deformation is chosen to be represented by the Hill48 yield criterion. This criterion allows the introduction of material anisotropy, which is interesting for sheet specimens, cut out of a cold rolled material. In an orthogonal coordinate system, based on the axes of orthotropy of the material the criterion can be written as:

$$\Phi = H(\sigma_x - \sigma_y)^2 + G(\sigma_x - \sigma_z)^2 + F(\sigma_y - \sigma_z)^2 + 2N\sigma_{xy}^2 + 2M\sigma_{xz}^2 + \sigma_{yz}^2 - 2\sigma_f^2 \quad (5)$$

in which  $\sigma_f$  represents the current flow stress and H, G, F, N and M define the form of the yield surface. The Hill48 quadratic yield criterion is a widely used yield criterion for the simulation of sheet metal material behavior. The plane of the sheet contains the x- and y-axis, while the z-axis is perpendicular to it. In that case the out of plane stresses  $\sigma_{xz}$ ,  $\sigma_{yz}$  and  $\sigma_z$  can be neglected, leading to a plane stress condition. Assuming this simplified stress situation, equation (5) reduces to:

$$\Phi = (G + H)\sigma_x^2 + 2H\sigma_x\sigma_y + (F + H)\sigma_y^2 + 2N\sigma_{xy}^2 - 2\sigma_f^2 \quad (6)$$

The parameters to be identified are F, G, H and N.

#### C. Hardening function

A hardening model is needed to represent the evolution of the yield surface during the process of plastic deformation. The type of hardening considered in the present study is a Swift type of isotropic hardening which describes the evolution of the yield surface size:

$$\sigma_f = \sigma_{y0} + K(\varepsilon_{eq}^{pl})^n \quad (7)$$

in which  $\sigma_f$  represents the actual flow stress,  $\sigma_{y0}$  is the initial yield stress and  $\varepsilon_{eq}^{pl}$  represents the equivalent plastic strain, which can be calculated using the following relation:

$$\varepsilon_{eq}^{pl} = \int_0^t \sqrt{\frac{2}{3} \left( (\dot{\varepsilon}_x^{pl})^2 + (\dot{\varepsilon}_y^{pl})^2 + (\dot{\varepsilon}_z^{pl})^2 + 2(\dot{\varepsilon}_{xy}^{pl})^2 \right)} dt \quad (8)$$

$\sigma_{y0}$ ,  $K$  and  $n$  are the three unknown parameters to be identified

#### IV. HOMOGENEOUS PARAMETER IDENTIFICATION

The orthogonal coordinate system defined for rolled material is based on three principal axes of that material, i.e. the rolling direction, the transverse direction and the normal direction. The local  $xyz$ -coordinate system for a tensile specimen cut out of a plate material is defined by the angle between the rolling direction and the specimens longitudinal axis defines. For a sheet metal sample, the  $x$ - and  $y$ -axis lie in the material plane and the  $z$ -axis is perpendicular to it.

Traditionally the parameters of the hardening law are determined based on a tensile test, performed on a specimen cut out in the rolling direction. The parameters of the Hill48 yield criterion on the other hand are determined by the Lankford coefficients  $r_{0^\circ}$ ,  $r_{45^\circ}$  and  $r_{90^\circ}$ . These coefficients represent the ratio between the transversal plastic strain rate and the through thickness plastic strain rate occurring during a tensile test in respectively the  $0^\circ$ ,  $45^\circ$  and  $90^\circ$  direction from the rolling direction. As the thickness strain cannot easily be measured, it is calculated using the assumption of volume conservation during plastic deformation. It can be shown that the relations between the Lankford coefficients and the different Hill48 parameters reduce to:

$$r_{0^\circ} = \frac{\dot{\varepsilon}_{y/0^\circ}^{pl}}{\dot{\varepsilon}_z^{pl}} = \frac{\dot{\varepsilon}_y^{pl}}{\dot{\varepsilon}_z^{pl}} = \frac{H}{G} \quad (9)$$

$$r_{90^\circ} = \frac{\dot{\varepsilon}_{y/90^\circ}^{pl}}{\dot{\varepsilon}_z^{pl}} = \frac{\dot{\varepsilon}_x^{pl}}{\dot{\varepsilon}_z^{pl}} = \frac{H}{F} \quad (10)$$

$$r_{45^\circ} = \frac{\dot{\varepsilon}_{y/45^\circ}^{pl}}{\dot{\varepsilon}_z^{pl}} = \frac{2N - F - G}{2(F + G)} \quad (11)$$

As the equivalent yield stress is equal to the stress in a uniaxial tensile test in the rolling direction, it can be stated that  $H+G=2$ . Together with this relation, equations 9-11 lead to a fully determined system of equations allowing to determine the four unknown parameters  $F$ ,  $G$ ,  $H$  and  $N$ .

Another possibility to identify the parameters of the yield criterion is by fitting the expression on a number of experimentally obtained stress states. To this end a number of standard tests can be performed: uniaxial tensile tests in the  $0^\circ$  and  $90^\circ$  direction from the rolling direction; plane strain tensile test; in plane equi-biaxial tensile test; pure shear test. The stress states corresponding to these tests can be represented in the  $\sigma_x - \sigma_y - \sigma_{xy}$ -space (fig.2). The axes correspond respectively to the stress in the rolling direction, the stress in the transverse direction and the shear stress. These stresses are not necessarily the principal stresses. This is only the case when the shear component is absent. Information about the experimental equipment that can be

used to attain the different stress states can be found in ref [9]. Results of this type of initial yield surface identification are discussed in refs.[10-11]. All of the performed experiments in these references possess the same property: the obtained strain field has to be as homogeneous as possible to allow a straightforward determination of the stress and the strain values. The hypothesis of homogeneity however, is not always verified.

Therefore, a method is proposed based on the coupling between Finite Element simulation and full-field surface displacement data. In this case the homogeneity of deformation is not longer needed, it is even avoided.

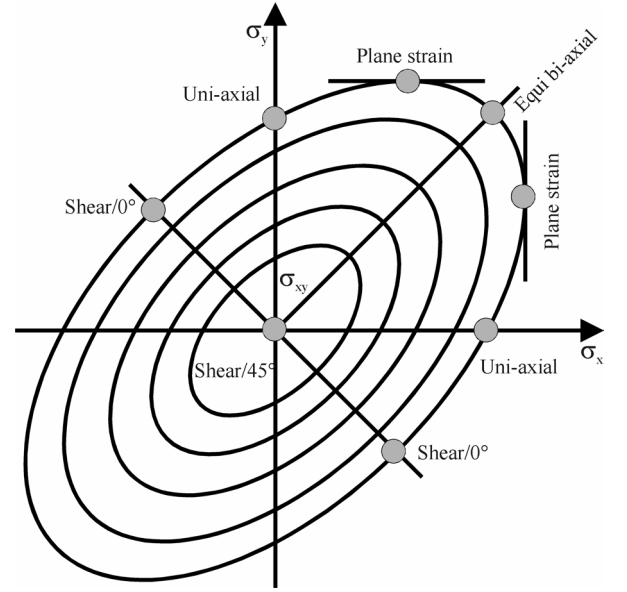


Figure 2: Different stress states on the initial yield surface expressed in the  $\sigma_x - \sigma_y - \sigma_{xy}$ -space defined by the axes of orthotropy

#### V. INVERSE MODELING

##### A. Introduction

A direct problem is the classical problem where a given experiment is simulated in order to obtain the final geometry of the specimen, the stresses and the strains. Inverse problems on the other hand are concerned with the determination of the unknown state of a mechanical system considered as a black box, using information gathered from the response to stimuli on the system [12].

The inverse problem is a problem where certain input data of the direct problem is deduced from the comparison between the experimental results and the numerical FE-simulation of that same problem. Not only the boundary information is used, but relevant information coming from local or full-field surface measurements is also integrated in the evaluation of the behavior of a given material. This type of parameter identification can also be found in refs. [13-14].

The values of the material parameters cannot be derived immediately from the experiment. A numerical analysis is necessary to simulate the actual experiment. However, this requires that the material parameters are known. The

identification problem can then be formulated as an optimization problem where the function to be minimized is some error function that expresses the difference between numerical simulation results and experimental data. In the present case the strains are used as output data. Figure 3 represents the flow-chart of the present inverse modeling problem.

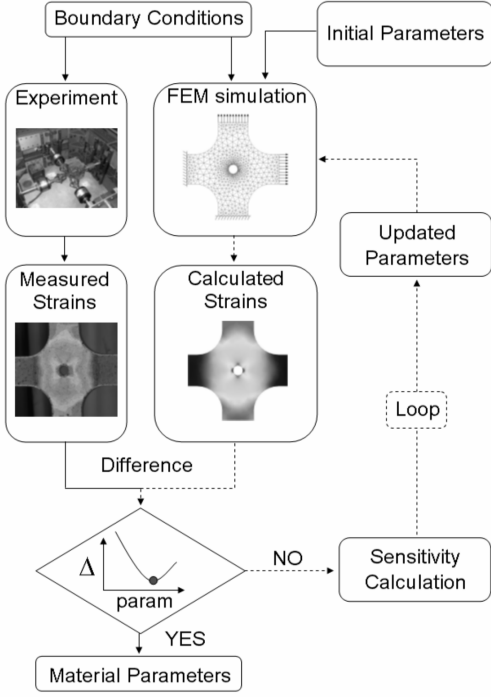


Figure 3: Inverse modelling flow-chart

### B. Optimisation and sensitivity calculation

Expression (12) shows the form of the least-squares cost function  $C(\underline{p})$  that is minimized, with  $\underline{p}$  the vector of material parameters to be identified. The residuals in the function are formed by the differences between the experimental and the numerical strains at every considered load step. The index “t” in expression (12) stands for the total number of elements and the index “s” stands for the total number of considered load steps.

$$C(\underline{p}) = \sqrt{\sum_{j=1}^s \left( \sum_{i=1}^t \left\langle \frac{\varepsilon_{x_i}^{\text{num}}(\underline{p}) - \varepsilon_{x_i}^{\text{exp}}}{\varepsilon_{x_i}^{\text{exp}}} \right\rangle^2 + \dots \right.} \\ \left. \frac{\left\langle \frac{\varepsilon_{y_i}^{\text{num}}(\underline{p}) - \varepsilon_{y_i}^{\text{exp}}}{\varepsilon_{y_i}^{\text{exp}}} \right\rangle^2 + \left\langle \frac{\varepsilon_{xy_i}^{\text{num}}(\underline{p}) - \varepsilon_{xy_i}^{\text{exp}}}{\varepsilon_{xy_i}^{\text{exp}}} \right\rangle^2}{j} \right) \quad (12)$$

The necessary condition for a cost function to attain its minimum is expressed by (13). The partial derivative of the function with respect to the different material parameters has to be zero:

$$\frac{\partial C(\underline{p})}{\partial p_r} = \frac{1}{C(\underline{p})} \sum_{j=1}^s \sum_{i=1}^t \left( \frac{\varepsilon_{x_i}^{\text{num}}(\underline{p}) - \varepsilon_{x_i}^{\text{exp}}}{\varepsilon_{x_i}^{\text{exp}}} \right) \frac{\partial \varepsilon_{x_i}^{\text{num}}}{\partial p_r} + \dots \\ \left( \frac{\varepsilon_{y_i}^{\text{num}}(\underline{p}) - \varepsilon_{y_i}^{\text{exp}}}{\varepsilon_{y_i}^{\text{exp}}} \right) \frac{\partial \varepsilon_{y_i}^{\text{num}}}{\partial p_r} + \left( \frac{\varepsilon_{xy_i}^{\text{num}}(\underline{p}) - \varepsilon_{xy_i}^{\text{exp}}}{\varepsilon_{xy_i}^{\text{exp}}} \right) \frac{\partial \varepsilon_{xy_i}^{\text{num}}}{\partial p_r} = 0 \quad (13)$$

By developing a Taylor expansion of the numerical (FEM) strains around a given parameter set, an expression is obtained in which the difference between the current parameters and their new estimates is given (14), m is the total number of parameters:

$$\varepsilon_i^{\text{num}}(\underline{p}) \cong \varepsilon_i^{\text{num}}(\underline{p}^k) + \sum_{j=1}^m \frac{\partial \varepsilon_i^{\text{num}}(\underline{p}^k)}{\partial p_j} (p_j - p_j^k) + \Theta^2 \quad (14)$$

When substituting this last expression into expression (13) and after rearranging some terms, the expression yielding the parameter updates is obtained (15):

$$\underline{\Delta p} = \left( \underline{S}^t \underline{S} \right)^{-1} \underline{S}^t \left( \underline{\varepsilon}^{\text{exp}} - \underline{\varepsilon}^{\text{num}}(\underline{p}^k) \right) \quad (15)$$

in which the following elements are:

- $\underline{\Delta p}$  : column vector of the parameter updates of  $\sigma_{y0}$ , K, n, G, F and N
- $\underline{\varepsilon}^{\text{exp}}$  : column vector of the experimental strains
- $\underline{\varepsilon}^{\text{num}}(\underline{p}^k)$  : column vector of the finite element strains as a function of the different parameters at iteration step k
- $\underline{p}^k$  : the three parameters at iteration step k
- $\underline{S}$  : Sensitivity matrix

$$\underline{S} = \begin{bmatrix} \frac{\partial \varepsilon_{x_1}^1}{\partial \sigma_{y0}} & \frac{\partial \varepsilon_{x_1}^1}{\partial K} & \frac{\partial \varepsilon_{x_1}^1}{\partial n} & \frac{\partial \varepsilon_{x_1}^1}{\partial G} & \frac{\partial \varepsilon_{x_1}^1}{\partial F} & \frac{\partial \varepsilon_{x_1}^1}{\partial N} \\ \frac{\partial \varepsilon_{y_1}^1}{\partial \sigma_{y0}} & \frac{\partial \varepsilon_{y_1}^1}{\partial K} & \frac{\partial \varepsilon_{y_1}^1}{\partial n} & \frac{\partial \varepsilon_{y_1}^1}{\partial G} & \frac{\partial \varepsilon_{y_1}^1}{\partial F} & \frac{\partial \varepsilon_{y_1}^1}{\partial N} \\ \frac{\partial \varepsilon_{xy_1}^1}{\partial \sigma_{y0}} & \frac{\partial \varepsilon_{xy_1}^1}{\partial K} & \frac{\partial \varepsilon_{xy_1}^1}{\partial n} & \frac{\partial \varepsilon_{xy_1}^1}{\partial G} & \frac{\partial \varepsilon_{xy_1}^1}{\partial F} & \frac{\partial \varepsilon_{xy_1}^1}{\partial N} \\ \vdots & \vdots & \vdots & \vdots & \vdots & \vdots \\ \frac{\partial \varepsilon_{xy_t}^1}{\partial \sigma_{y0}} & \frac{\partial \varepsilon_{xy_t}^1}{\partial K} & \frac{\partial \varepsilon_{xy_t}^1}{\partial n} & \frac{\partial \varepsilon_{xy_t}^1}{\partial G} & \frac{\partial \varepsilon_{xy_t}^1}{\partial F} & \frac{\partial \varepsilon_{xy_t}^1}{\partial N} \\ \vdots & \vdots & \vdots & \vdots & \vdots & \vdots \\ \frac{\partial \varepsilon_{xy_t}^s}{\partial \sigma_{y0}} & \frac{\partial \varepsilon_{xy_t}^s}{\partial K} & \frac{\partial \varepsilon_{xy_t}^s}{\partial n} & \frac{\partial \varepsilon_{xy_t}^s}{\partial G} & \frac{\partial \varepsilon_{xy_t}^s}{\partial F} & \frac{\partial \varepsilon_{xy_t}^s}{\partial N} \end{bmatrix} \quad (16)$$

The sensitivity matrix groups the sensitivity coefficients of the strain components in every element of the FE mesh and

for every considered load step with respect to the different material parameters.

$\frac{\partial \varepsilon_{xy}^s}{\partial n}$ , in expression 16, is the partial derivative of the shear strain component of element number “t” at load step “s” with respect to parameter “n”.

## VI. IDENTIFICATION USING SIMULATED STRAIN FIELDS

### A. Finite element simulation

In order to test the proposed routine, a virtual experiment is set up. The specimen geometry which is chosen is shown in figure 4 (lower part). It has a thickness of 1mm. The reason for the hole in the specimen is the following: the aim is to localise the plastic deformation in the central part of the specimen where a biaxial stress and strain state exists. For the identification of the parameters of the hardening law, this may not be really necessary. However, for the identification of anisotropic yield criteria, it is mandatory to obtain non-uniaxial plastic deformation.

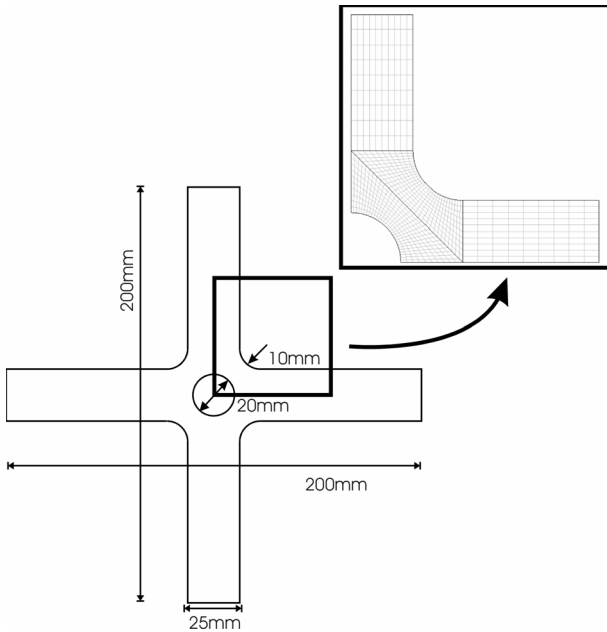


Figure 4: Geometry (left) and FE-mesh (right) of the cruciform specimens

The FE-simulation on the other hand is performed on a quarter of the piece, assuming symmetrical loading conditions. Figure 4 (upper part) shows an image of the FE-mesh. The simulation is force driven, as in actual experimental settings forces will be measured as well. The boundary conditions are the following: The left-hand side of the specimen is rigidly fixed in the horizontal direction and freely supported in the vertical direction. The bottom of the specimen on the other hand is fixed in the vertical direction and freely supported in the perpendicular direction. The tensile forces are uniformly applied over the top and right-hand side section of the specimen. The simulations are performed assuming plane stress conditions. This is an acceptable hypothesis given the thickness of the specimen.

The FE-mesh is made up out of isoparametric quadrilateral Lagrange elements of the second order.

The total force applied in the horizontal as well as in the vertical direction is equal to 1000N. This is an arbitrary value to permit the existence of plastic deformation on the one hand and to limit the CPU-time for a simulation on the other hand. The force is applied in twelve equal load steps. The numerical model assumes a linear isotropic elastic behaviour with a E-modulus of 210 GPa and a Poisson’s ratio of 0.33.

Figures 5 and 6 show the representation of the different stress states in the  $\sigma_x - \sigma_y - \sigma_{xy}$ -space for the elements in which plastic deformation occurs first. These figures are analogous to the representation shown in figure 2. The difference is that in this case the different stress states are present in the same experimental set-up.

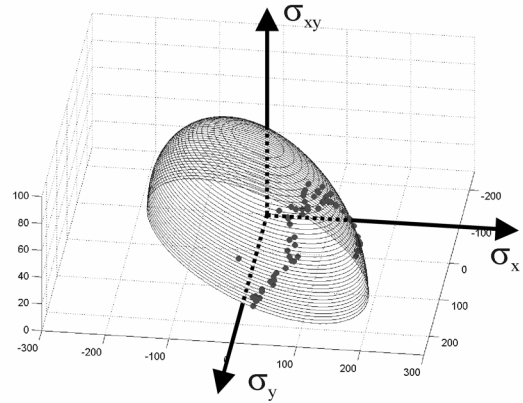


Figure 5: Stress states present in a biaxially loaded specimen and lying on the initial yield surface (perspective view)

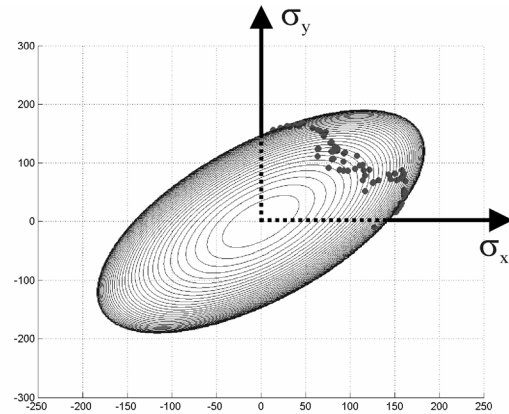


Figure 6: Stress states present in a biaxially loaded specimen and lying on the initial yield surface (top view)

### B. Identification Results

The increments used for the forward difference calculation of the sensitivities of the different total strain values  $\varepsilon_x$ ,  $\varepsilon_y$  and  $\varepsilon_{xy}$  for the respective parameters are the following:  $d\sigma_{y0}=0.1$ ;  $dK=1$ ;  $dn=0.01$ ;  $dF=dG=dN=0.01$ . Only the ten

last load steps are used in the identification procedure. The load steps in which no plastic deformation occur are not considered as the sensitivities with respect to the different parameters in that case equal zero. The constraints used in the optimisation routine are the following:  $H+G=2$ ;  $\sigma_{y0} \geq 0$ ;  $K \geq 0$ ;  $F \geq 0$ ;  $G \geq 0$ ;  $N \geq 0$ .

The virtual experimental strain values according to the last ten load steps are obtained based on a simulation run with the reference values in table 1. The starting values of the identification procedure are shown in table 1 as well.

Figures 7-10 represent the different parameter values corresponding to every iteration step in the optimisation routine. The optimisation has been stopped at the ninth iteration step.

TABLE I

REFERENCE AND STARTING VALUES FOR THE NUMERICAL VALIDATION

	$\sigma_{y0}$ MPa	K	n	F	G	N
Reference val.	100	1000	0.8	0.64	0.78	2.82
Starting val.	90	1500	0.7	1	1	1

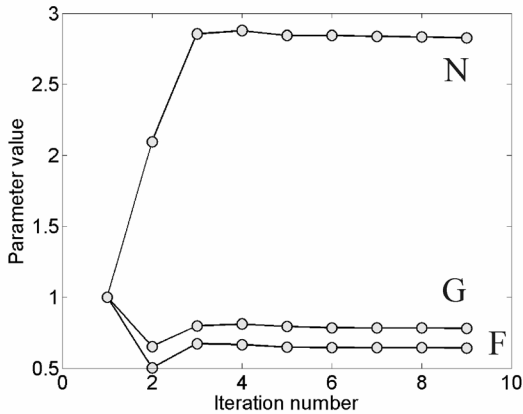


Figure 7: Parameter values of F, G and N in function of the iteration step

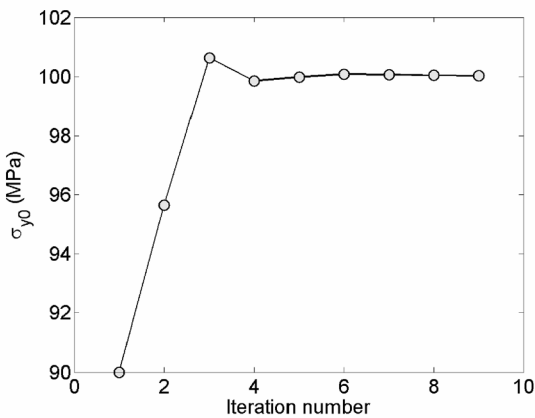


Figure 8: Parameter value of  $\sigma_{y0}$  in function of the iteration step

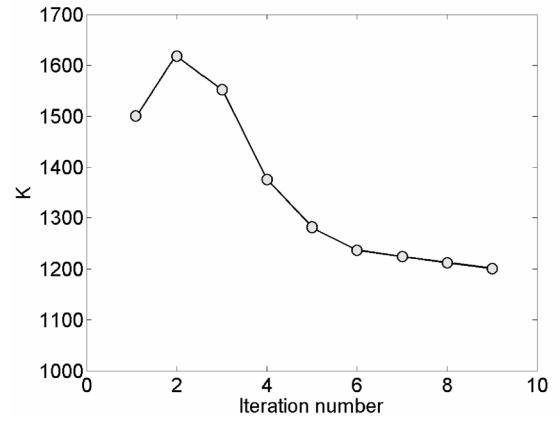


Figure 9: Parameter value of K in function of the iteration step

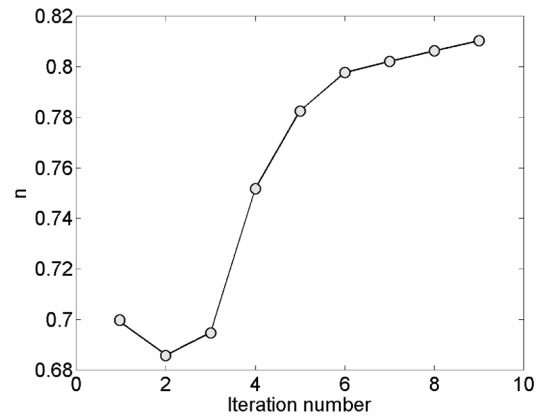


Figure 10: Parameter value of n in function of the iteration step

The results show that the values of  $\sigma_{y0}$ , F, G and N are attained at an early stage. For the values of K and n however, more iterations are needed. The parameter “n” influences the hardening curve at the onset of plastic deformation, whereas the parameter “K” becomes more important for larger deformations. As the deformations achieved in the present simulations are not that important, the routine has difficulties finding the correct value of K. As both parameters are coupled by the same hardening law, the process has some difficulties finding the right value for n as well.

It has also been found that the value of the starting parameters does not affect the final and optimal parameter values.

## VII. CONCLUSION

A method has been proposed to determine the parameters ( $\sigma_{y0}$ , K and n) of a Swift type of isotropic hardening law. The method is based on the inverse modeling of a perforated cruciform specimen under biaxial tension. A least-squares formulation of the difference between the experimental and the numerical strains is used along with a constrained Newton-type algorithm in the optimization process. A virtual experiment, in which the material parameters are known, is

used to check the routine and to analyze the influence of the starting values on the obtained parameter estimates.

It is shown that numerically the biaxial tensile test on the perforated cruciform specimen contains enough information for the different Hill48 yield surface to be identified. The parameters of the Swift type of isotropic hardening law can be identified as well, however the deformation should be more important to limit the number of iterations until convergence of those parameters.

Future work consists in studying the sensitivity of the obtained parameter values to noise on the measured strain values. In the near future, real biaxial tensile tests will be performed on metal cruciform specimens, on which the measurements will be performed by digital image correlation.

#### ACKNOWLEDGEMENTS

This project is supported by the Belgian Science Policy through the IAP P05/08 project.

#### REFERENCES

- [1] Ghouati O., Gelin J.C., Identification of material parameters directly from metal forming processes. *Journal of materials processing Technology*, Vol 80-81,560-564, 1998
- [2] Kucharski S., Mróz Z., Identification of plastic hardening parameters of metals from spherical indentation tests, *Materials science and engineering A*, Vol 318, 65-76, 2001
- [3] Springmann M., Kuna M., Identification of material parameters of the Rousselier model by non-linear optimization, *Computational materials science*, Vol 26, 202-209, 2003
- [4] Zouani A., Bui-Quoc T., Bernard M., A proposed device for biaxial tensile fatigue testing, *Fatigue and Fracture-1996*, ASME PVP-323, vol. 1, p. 331-339, 1996
- [5] Dawicke D.S., Pollock W.D., Biaxial testing of 2219-T87 aluminum alloy using cruciform specimens, *Nasa Contractor Report 4782*, p. 1-46
- [6] Chaudonneret M., Gilles P., Labourdette R., Policella H., *Machine d'essais de traction biaxiale pour essais statiques et dynamiques*, La Recherche Aérospatiale, vol. 5, p. 299-305, 1977
- [7] Makinde A., Thibodeau L., Neale K.W., Development of an apparatus for biaxial testing using cruciform specimens, *Experimental mechanics*, vol. 32/2, p. 138-144, 1992
- [8] Lecompte D., Smits A., Sol H., Vantomme J. and Van Hemelrijck D., Elastic orthotropic parameter identification by inverse modelling of biaxial tests using Digital Image Correlation, 8<sup>th</sup> European Mechanics of Materials Conference on Material and structural identification from full-field Measurements Cachan – France 13-15 Sep, 2005
- [9] P. Flores. Development of experimental equipment and identification procedures for sheet metal constitutive laws. PhD thesis, University of Liège, 2006.
- [10] P. Flores, L. Duchêne et al. Model identification and FE simulations : Effect of different yield loci and hardening laws in sheet forming. Proceedings of the 6<sup>th</sup> Numisheet Conference, Detroit, Michigan, USA, 2005, p.371-381
- [11] H. Vegter, C. ten horn et al. Characterisation and modeling of the plastic material behaviour and its application in sheet metal forming simulation. Proceedings of COMPLAS VII, Barcelona, 2003.
- [12] Bui, H.D., *Inverse Problems in the Mechanics of Materials: An Introduction*, CRC Press, Inc., Florida, 1994
- [13] Kajberg, J. and Lindkvist, G. 2004. Characterisation of materials subjected to large strains by inverse modelling based on in-plane displacement fields. *International Journal of Solids and Structures* Vol 41, No 13, 3439-3459
- [14] A.Khalfallah, H. BelHadjSalah, A. Dogui. Anisotropic parameter identification using inhomogeneous tensile test. *European journal of Mechanics A/Solids*, 2002;21:927-942